Combustion Science and Technology
Publication details, including instructions for authors and subscription information:
http://www.informaworld.com/smpp/title~content=t713456315

Numerical Study of Thermal-Diffusive Instability of Premixed Flames

Bruno Denet[a]; Pierre Haldenwang[a]
[a] Laboratoire de Recherche en Combustion, Université de Provence/CNRS, Marseille Cedex 13, France

To cite this Article Denet, Bruno and Haldenwang, Pierre(1992) 'Numerical Study of Thermal-Diffusive Instability of Premixed Flames', Combustion Science and Technology, 86: 1, 199 — 221
To link to this Article: DOI: 10.1080/00102209208947195
URL: http://dx.doi.org/10.1080/00102209208947195

Combust. Sci. and Tech., 1992, Vol. 86, pp. 199–221
Photocopying permitted by license only

Numerical Study of Thermal-Diffusive Instability of Premixed Flames

BRUNO DENET and PIERRE HALDENWANG *Laboratoire de Recherche en Combustion, Université de Provence/CNRS. Centre de Saint Jérôme (S 252), 13397 Marseille Cedex 13, France*

(*Received February 28, 1991; in final form October 17, 1991*)

Abstract—The 2-D thermal-diffusive model of premixed flames is solved numerically. The growth rates of the thermal-diffusive instability are compared to the linear theory. It is shown that the discrepancy, although large (a relative error than can be larger than 100%), behaves like $O(1/\beta)$ as expected by asymptotics (β being the reduced activation energy or Zeldovich number). We additionally present results far in the non-linear domain. They exhibit turbulent behaviour which are qualitatively similar to the dynamical properties of the Kuramoto–Sivashinsky model-equation.

Key words: thermal-diffusive instability, wrinkled premixed flame, turbulent flame, numerical combustion.

1 INTRODUCTION

Plane flames rarely exist. The interface between (cold) fresh gases and (hot) combustion products is indeed subject to instabilities leading to well-known patterns of wrinkled flames—for recent reviews see Sivashinsky (1983), Williams (1985), Clavin (1985). Two different mechanisms are usually advanced: the Darrieus–Landau instability and the thermal-diffusive instability. The first one is of hydrodynamic origin and is caused by density changes across the flame. Estimates (at least at the leading order) can be provided without requiring the study of internal profile of the premixed flame. On the contrary, the thermal-diffusive instability is a consequence of the competition between diffusive phenomena through the premixed flame thickness. Hence, the predictions require to take into account reaction-diffusion effects inside the flame thickness.

Furthermore, when finite flame thickness is taken into account in the study of Darrieus–Landau instability, first order corrections obtained by asymptotic analysis and by multi-scale analysis (Clavin and Williams 1982 or Pelcé and Clavin 1982) have shown that thermal-diffusive effects play a stabilizing role for common values of gas expansion. This result shows that the thermal-diffusive instability is actually limited to a restricted range of premixed flames: flames having small gas expansion or very low Lewis number.

Numerical investigations are usually expected either to provide predictions well beyond the scope of the theoretical approach or to check the quality of basic assumptions underlying the theory. More precisely, the above mentioned theoretical studies of the Darrieus–Landau instability contain two basic ingredients: asymptotic analysis founded on the fact that the activation energy is high and multi-scale analysis based on scale separation between flame thickness and size of cells. Complete checking of both assumption and providing of non-linear results is the purpose of a forthcoming paper (Denet and Haldenwang 1991).

Even if the thermal-diffusive instability can only occur at low gas expansion (in plane geometry), it nevertheless represents an interesting physical framework in which the asymptotic assumption can be properly checked. The theoretical study of the threshold of the thermal-diffusive instability is indeed exact in the sense that no scale

separation between flame thickness and cell size is required. Checking the quality of the asymptotic expansion is one of the two purposes of the present paper.

The second purpose concerns physical behaviours far from the threshold. As observed in experiments (Bregeon *et al.* (1978), Sabathier *et al.* (1981), Quinard *et al.* (1984)), the flames in the unstable regime are wrinkled, exhibiting cell patterns which become more and more cusped as the non-linearity increases. Far in the non-linear domain, this interface undergoes turbulent fluctuations: cusped forms continuously appear or merge in a chaotic way. On the other hand, such effects have been widely observed in numerical computation of a model-equation describing the thermal-diffusive instability: the well known Kuramoto-Sivashinsky equation (see for instance Hyman and Nicolaenko (1986), Frisch *et al.* (1986)). The qualitative agreement between experimental observations and the Kuramoto–Sivashinsky model-equation (proposed as a model of self-turbulizing flame and hereafter referred as KS equation) asks the following question: does the thermal-diffusive model (from which the KS equation is derived) already contain such a physics or is the agreement fictitious? To answer this question is the subject of the second contribution of the present paper.

So, this paper presents two-dimensional numerical simulations of premixed flame propagation in the framework of the thermal-diffusive model (see Barenblatt *et al.* (1962)). We will provide quantitative comparisons between numerically measured growth rates and those furnished by the linear asymptotic theory (Sivashinsky 1977). Then, we shall simulate turbulent behaviours which will be qualitatively compared to the results of the KS equation.

Several numerical simulations of the thermal-diffusive model, or related models, have been recently carried out and can be found in Guillard *et al.* (1987), Denet & Haldenwang (1989), Bayliss *et al.* (1989). It has been suggested in Kailasanath *et al.* (1989) that the thermal-diffusive instability was a plausible explanation of cellular structures in lean hydrogen–oxygen premixed flames. These authors report numerical simulations of such flames.

A lot of theoretical works have been performed using thermal-diffusive approximations in various combustion problems. For instance, the case of burner-anchored flames is studied in MacIntosh and Clarke (1984) and the case of solid propellant flames in Maroglis and Williams (1989).

The paper is organized as follows. In Section 2 we briefly recall the constant-density model and some of its theoretical properties concerning the stability of the plane thermal-diffusive flame. In Section 3 we present the numerical method we use. Section 4 is devoted to the presentation of a set of numerical results concerning the growth rates of the thermal-diffusive instability. In Section 5 we present non-linear solutions, including the case of a self-turbulizing flame.

2 PHYSICAL MODEL AND THEORETICAL RESULTS

As mentioned in the introduction, we are presently interested in the thermal-diffusive instability. In the limit of small gas expansion it has been shown by Sivashinsky (1977) that such an instability, caused by the destabilizing influence of the diffusion of limiting species, is driven by the so-called thermal-diffusive model. This model of premixed flames (Barenblatt *et al.* (1962)) assumes that the gas expansion plays a negligible role. Strictly speaking, this is only true for flames in which the fresh mixture (although frozen) has a temperature of the same order as the flame temperature. However, in most applications, the gas density is generally much lower in the burnt gases than in the fresh mixture. And, as recalled above, important hydrodynamical

effects, as the Darrieus–Landau instability, are thus not included in the thermal-diffusive model.

Because the present simulations will lead to a large amount of computation, we choose the simplest chemistry: a single one-step chemical reaction is assumed. Non-dimensional quantities are obtained using a classical approach: the length scale is the flame thickness obtained from asymptotics, likewise the velocity unit is the asymptotic flame speed. The use of the normalized variables allows us (see *e.g.*, Clavin (1985), Buckmaster and Ludford (1983)) to write the model, in a frame moving with the flame front, as follows:

$$\frac{\partial T}{\partial t} + U\frac{\partial T}{\partial x} = \Delta T + \Omega \tag{2.1a}$$

$$\frac{\partial C}{\partial t} + U\frac{\partial C}{\partial x} = \frac{1}{\mathrm{Le}}\Delta C - \Omega \tag{2.1b}$$

with

$$\Omega = \frac{\beta^2}{2\mathrm{Le}} C \exp\left(\frac{\beta(T-1)}{1+\gamma(T-1)}\right) \tag{2.2}$$

where Δ is the Laplacian, T and C correspond to the reduced temperature of the gas mixture and concentration of a reactant (the other reactant being in excess). Le, β and γ are respectively the Lewis number of the reactant (defined as the ratio of the thermal to the molecular diffusivity), the reduced activation energy (or Zeldovich number) and the heat release parameter. U is the reduced flame speed which is an unknown of the problem. U is supposed to be parallel to the x-direction.

Because we are interested in the resolution of unstable flame fronts, we shall assume that the flat front is unstable with respect to patterns, periodic in y (the direction perpendicular to the flame speed). Thus the boundary conditions read:

$$T(x = -\infty, y) = 0, \quad T(x = +\infty, y) = 1 \tag{2.3(a–b)}$$

$$C(x = -\infty, y) = 1, \quad C(x = +\infty, y) = 0 \tag{2.3(c–d)}$$

$$T(x, y = -Y_0) = T(x, y = +Y_0),$$

$$\frac{\partial T}{\partial y}(x, y = -Y_0) = \frac{\partial T}{\partial y}(x, y = +Y_0) \tag{2.4(a–b)}$$

$$C(x, y = -Y_0) = C(x, y = +Y_0),$$

$$\frac{\partial C}{\partial y}(x, y = -Y_0) = \frac{\partial C}{\partial y}(x, y = +Y_0) \tag{2.4(c–d)}$$

Starting from this model, the theoretical analysis is classically carried out by means of an asymptotic analysis in powers of β^{-1} (β being supposed to be large) which assumed that the flame characteristics can satisfy the near equi-diffusion limit:

$$\mathrm{Le} - 1 \approx O(\beta^{-1}) \ll 1 \tag{2.5}$$

From a linear point of view, such an analysis leads (see Sivashinsky (1977)) to the

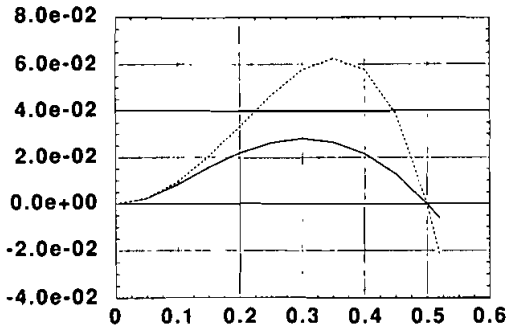

FIGURE 1 Theoretical growth rates *vs.* wave vector for $l = -4$: complete dispersion relation (continuous line) and expansion in powers of k (dotted line).

following dispersion relation characterizing the growth rate of sinusoidal perturbations of wave-length k:

$$(1 - \Gamma)\Gamma^2 = (-l/2)(1 - \Gamma + 2\sigma) \tag{2.6}$$

where

$$\Gamma = \sqrt{1 + 4(\sigma + k^2)}$$

where σ is the growth rate, k is the wave vector, l is the control parameter defined by $l = \beta(\mathrm{Le} - 1)$.
For k small, this formular can be expanded in powers of k

$$\sigma = -\left(1 + \frac{\beta}{2}(\mathrm{Le} - 1)\right)k^2 - 4k^4 \tag{2.7}$$

The threshold of the diffusive thermal instability is given by

$$l = \beta(\mathrm{Le} - 1) < -2 \tag{2.8}$$

Note that the complete formula of growth rates (Eq. 2.6) and its approximation for small k (Eq. 2.7) are rather different, as shown in Figure 1, where these two dispersion relations are plotted for $l = -4$. We can see on this plot that the agreement between the two formulas is limited to k below 0.1, the maximum being very different in both cases. They however contain qualitatively the same physics because they have the same unstable band. Nevertheless, because a quantitative point of view is here taken, we will never use the simplified dispersion relation in this paper. In the following, numerical growth rates will be compared to the exact dispersion relation (Eq. 2.6). Recall that this relation is the leading term of an expansion in the powers of β^{-1}: there should be an agreement between theory and numerical experiments only for sufficiently high β. At this point, it can be noted that the dispersion relation does not contain the parameter γ: this parameter has no influence on the leading term of the expansion in powers of β^{-1}. The numerical results will show that this parameter has important effects on the following terms.

When l is near its critical value -2, it has been shown that a non-linear equation, the KS equation, characterizing the front position can be derived from asymptotics.

The linear part is directly connected to the simplified dispersion relation. As for the non-linear term, it corresponds to a geometrical effect, expressed at the lowest order in term of α, the amplitude of the front perturbation. The equation can read:

$$\alpha_t + \tfrac{1}{2}\alpha_y^2 + \alpha_{yy} + \alpha_{yyyy} = 0 \tag{2.9}$$

This 1-D equation corresponds to the position of a 2-D flame front. The present form of the equation has been obtained after some rescaling. The control parameter now appears as the size of the integration domain. We note that the thermal-diffusive instability occurs as a local effect: only derivatives of the local front position are present in the KS equation. Numerical experiments on this equation have shown that the plane flame evolves into cellular patterns, the characteristic wave-number of which is somewhat smaller that the wave vector corresponding to the maximum growth rate. The resulting cell pattern is essentially unsteady with a rich set of time-dependent behaviour (see *e.g*, Hyman *e.g.* (1986)). In fact, we will obtain here comparable results showing that, at least in a qualitative sense, the actual validity domain of the KS equation is larger than the one supposed by the asymptotic derivation.

3 THE NUMERICAL ALGORITHM

In contrast to the above mentioned asymptotic analyses, we now consider a numerical description analysing the flame up to its smallest length scales. Generally this type of simulation requires (see *e.g.*, Benkhaldoun and Larrouturou (1990), Smooke and Koszykowski (1986)) special ingredients such as self-adaptive gridding. This is due to the fact that three different length scales are present in the computational domain. The smallest one is related to the reaction zone, the second being the length scale of the pre-heating region. The largest one is scaled by the typical wave-length of the wrinkles. The first two length scales are in the direction perpendicular to the flame surface while the third one is parallel to the front. But, because large cusps are expected in the non-linear range, the last typical length also scales the amplitude of the interface fluctuations. Clearly, this is a third length scale in the direction perpendicular to the flame front, indicating the minimum size of the domain in which the numerical study have to track the flame. In conclusion, large wrinkles require a real 2D self adaptive gridding, moving in phase with the corrugated flame. In fact, this is a huge numerical task and so expensive in CPU time that practical running seems to be limited.

To overcome these problems, we here use a different approach. We first state that scale representation of three orders of magnitude stays within the scope of Fourier spectral methods (Canuto *et al.* 1988). Using these type of methods, we can renounce to implement a scheme that adapts the gridding according to the successive flame positions. However, making use of efficient Fourier spectral methods requires one to transform a non-periodic problem into a periodic one in all directions. We now summarize the main points of the method (see Denet and Haldenwang (1989) for more details).

From the point of view of temporal discretisation, we have used either a first order or second order scheme. The production term being taken explicitely, stability requirements imposes in any case small time steps. That is the reason why we have not seen much differences between first and second order in the time when measuring growth rates: the difference can be of the order of 5% in the worst cases, the second order value being generally a little higher. The second order scheme being approximately twice as expensive as the first order one (the time step being further reduced), in most results presented here, the first order scheme is used.

We are interested in the computation on the $(-X_0, X_0)*(-Y_0, Y_0)$ rectangle with periodic boundary conditions in the y-direction. In the x-direction the boundary conditions are:

$$T(x = -X_0, y) = 0, \quad T(x = X_0, y) = 1;$$

$$C(x = -X_0, y) = 1, \quad C(x = X_0, y) = 0 \qquad (3.1(a\text{–}d))$$

Strictly speaking such boundary conditions should be imposed at infinity. Nevertheless, if X_0 is large enough, these boundary conditions can be satisfied at finite distances without loss of accuracy (except at vanishing wavenumbers as discussed in the next paragraph).

Taking into account these non-periodic boundary conditions, let us define θ and ψ as the following intermediate unknowns:

$$T(x, y) = S_0(x) + \theta(x, y) \qquad (3.2a)$$

$$C(x, y) = 1 - S_0(x) + \psi(x, y) \qquad (3.2b)$$

where $S_0(x)$ is a smooth "step" function going from 0 to 1 with zero slopes at both ends. Among the functions satisfying these conditions we have chosen the following one:

$$S_0(x) = \frac{1}{2}\left[1 + \tanh\left(\Gamma \tan\left(\frac{z - \pi}{2}\right)\right)\right] \qquad (3.3)$$

where $z = (x + X_0)\pi/X_0$ and Γ is a parameter that determines the slope of S_0 at the centre of the integration domain.

If we suppose X_0 large enough we can then assume all the x-derivatives of $T(x, y)$ and $C(x, y)$ to be negligible at $x = \pm X_0$. Hence it is straightforward to show that $\theta(x, y)$ and $\psi(x, y)$ are periodic in all directions, likewise their derivatives. Because the physics of the flame considers that Ω, the production term, has a small support of order $1/\beta$, then Ω and its further derivatives vanish at $x = \pm X_0$. The thermal-diffusive model is thus posed in terms of a periodic problem having excellent properties of convergence in the framework of Fourier spectral methods: exponential convergence to the exact solution can be achieved because all quantities (and their further derivatives) are periodic in all directions. Nevertheless, as mentioned before the present method is not an adaptive one so that we generally need several hundred collocation points at least in the x-direction.

4 COMPUTATION OF LINEAR GROWTH RATES OF THE THERMO-DIFFUSIVE INSTABILITY

4.1 *Additional Numerical aspects*

In order to compute growth rates, we take as initial condition a sinusoidal flame of low amplitude (10^{-5} in units of flame thickness). After some transient the amplitude begins to grow exponentially: we have actually measured the growth rate of several norms (in the x direction) of the Fourier components (partially obtained in the y direction) corresponding to the sine wave we have introduced as initial condition. The results do not depend on the selected norm.

By contrast, X_0 the size of the integration domain is a very sensitive quantity, especially at low wavenumbers. As a result, if X_0 is not large enough, the linear growth rate does not vanish as k tends to zero. In order to limit the number of collocation points required when X_0 is large, we took advantage of the fact that the sinusoidal flame, in the linear growth stage, is nearly plane. Then, we can use, for this linear study, a mapping which increases the precision in the reaction zone. It transforms x, the physical coordinate, to x', the new coordinate defined from $-\pi$ to π (y being unchanged) by the formula.

$$x' = \pi \frac{x/a}{\sqrt{1 + (b - 1) \tanh ((x/c)^2) + (x/a)^2}}$$

where $b = (a_i/a)^2$; a, a_i and c are parameters controlling the position of the points in physical space. The meaning of the parameters is the following: for x small ($x \ll c$), we have essentially

$$x' \approx \pi \frac{x/a}{\sqrt{1 + (x/a)^2}} \approx \pi(x/a)$$

On the contrary, for $x \gg c$, the relation between x' and x becomes

$$x' \approx \pi \frac{x/a_i}{\sqrt{1 + (x/a_i)^2}}$$

these two relations are equally valid for $x < 0$. To sum up, for x small, the change of variable is controlled by a; the smaller a is, the more adapted near $x = 0$ the mesh is. For x large, the change of variable is controlled by a_i; the greater a_i is, the more distant from $x = 0$ the points are. The transition region occurs around $x = c$.

In our numerical measurement of growth rates we take, *e.g.*, for $\beta = 10$, 256 modes in the x direction, $a = 7$, $a_i = 15$ and $c = 8.5$. When β increases, we reduce a and a_i, keeping the same value for the other parameter c, in order to adequately resolve the reaction zone, which is smaller when β is great.

4.2 *A Secondary Effect Due to the Gas Expansion*

The thermal-diffusive theory is derived in the limit $\gamma \ll 1$; *i.e.*, vanishing gas expansion. As mentioned in Section 2, this hypothesis allows one to separate the equations for temperature and concentration from the hydrodynamical ones.

Now suppose this separation holds and we want to check the quality of asymptotics applied to real flames. The gas expansion parameter still appears in the production term (Eq. 2.2) and can modify the internal heat release profile. According to asymptotics, this "side" effect is feeble (see Joulin and Clavin (1979)). Equation 2.6 is indeed independent of γ and this parameter is expected to appear in the correction of the leading order.

As it will be shown in the next paragraph, this correction for real flames is however very large. Hence, we have to try to estimate its dependency on γ. In Table I, we actually show that the influence of the parameter γ on the growth rates is very important. In the unstable case $l = -2.5$, $\beta = 10$, and for different values of k, this table provides the values of numerical growth rates for $\gamma = 0.8$ and $\gamma = 0.4$. For the value $\gamma = 0.8$, characteristic of real flames, the discrepancy between theory and

TABLE I
$\sigma_{exp}(\gamma = 0.08)$, $\sigma_{exp}(\gamma = 0.4)$, σ_{th} *vs.* k, for $l = -2.5$ and $\beta = 10$

k	$\sigma_{exp}(\gamma = 0.8)$	$\sigma_{exp}(\gamma = 0.4)$	σ_{th}
0.1	6.50×10^{-3}	4.67×10^{-3}	1.91×10^{-3}
0.2	1.40×10^{-2}	9.64×10^{-3}	2.60×10^{-3}
0.3	1.07×10^{-2}	5.15×10^{-3}	-5.50×10^{-3}

numerics is larger than for $\gamma = 0.4$. As we want to test the validity of asymptotics for real flame, we will essentially study the value $\gamma = 0.8$ in what follows; $\gamma = 0.8$ is a typical value in the experiments and the most often used in numerical simulations (see Peters and Warnatz (1982)). Note that a small value for γ makes the problem steeper and then closer to asymptotics, so that the value $\gamma = 0$ induces numerical difficulties.

4.3 *Numerical Results*

We have numerically measured the growth rates in the several cases $l = -4$ (very unstable case), $l = 2.5$ (unstable case), $l = -1.5$ (stable case) and for different values of β, from $\beta = 10$ (a realistic value and considered usually to be sufficiently high for the theory to apply), up to the very high, unrealistic value $\beta = 30$. Our measurements concern $\gamma = 0.8$ and point out that the variations of the results with respect of β (for fixed l) is important.

In Figure 2, the case $l = -4$ is considered. The theoretical dispersion relation, and the numerical dispersion relations obtained for $\beta = 10$ and $\beta = 20$, are plotted. It can be observed that a close agreement between theory and numerics is recovered only for sufficiently high values of the wave vector k (these values do not lead to instabilities). This comparison is still meaningful at large wavenumber because the theory to which we compare our results is a complete theory, non-perturbative in k.

Nevertheless, the interesting range for the comparison is the one where growth rates are positive. Figure 3 is an enlargement of Figure 2 in the domain of wave vectors where the growth rate remains positive. The difference between theory and numerical experiment is actually large. For real flames ($\beta = 10$), the maximum discrepancy exceeds 100%. The limit of the unstable band ($k = 0.6$) is relatively near the theoretical

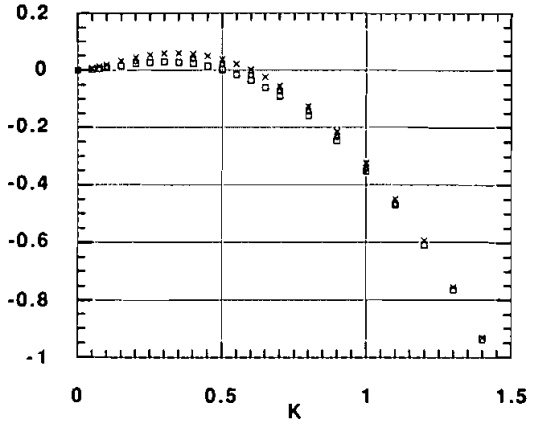

FIGURE 2 Growth rates *vs.* wave vector for $l = -4$ $\gamma = 0.8$: theory (squares); $\beta = 10$ (crosses); $\beta = 20$ (diamonds).

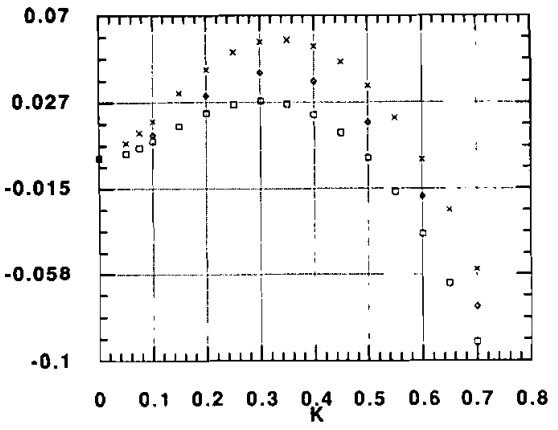

FIGURE 3 Enlargement of Figure 2 in the domain of unstable wave vectors.

value ($k = 0.5$), but the maximum is twice as large as the predicted value. In the case of $\beta = 20$ the dispersion relation gets nearer the theoretical curve and allows more confidence in the asymptotic results.

It could be argued that the value $l = -4$ is too far from the threshold and poorly satisfies the hypothesis $l = O(1)$. So that, the discrepancy observed could be easily explained. In Figure 4, we now take $l = -2.5$; the lack of agreement is even worse: both on the size of the unstable domain and on the position of the maximum. Actually the observed differences in the value of the growth rate are less than that for $l = -4$ in absolute value, but greater in terms of relative difference: for instance the maximum for $\beta = 10$ is five times as large as the predicted one. It can be explained in the following way: for finite β, the stability limit is not located exactly at $l = -2$, so that the relative error becomes amplified near the theoretical threshold. For larger k, agreement between theory and numerical experiment is recovered, but it occurs only at negative growth rates and is not plotted on Figure 4.

In Figure 5, the case $l = 1.5$ is considered; although this is a stable case, differences

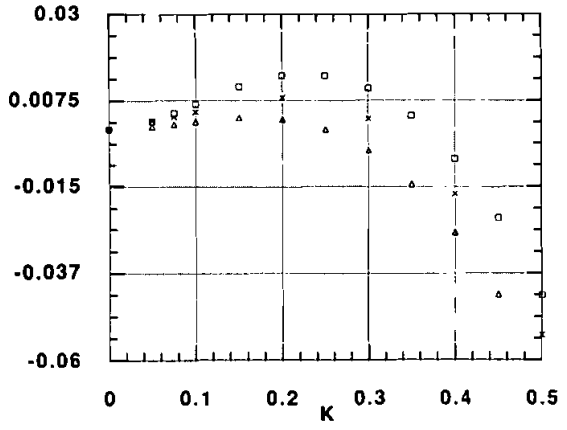

FIGURE 4 Growth rates *vs.* wave vector for $l = -2.5$ $\gamma = 0.8$: theory (triangles); $\beta = 10$ (squares); $\beta = 20$ (crosses).

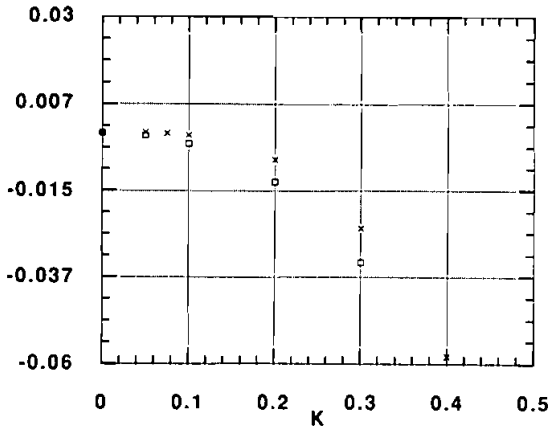

FIGURE 5 Growth rates *vs.* wave vector for $l = -1.5$ $\gamma = 0.8$: theory (squares); $\beta = 10$ (crosses).

are still important. In Figure 6, the difference between theory and numerical experiment is plotted *vs.* k ($\beta = 10$ fixed) and for the three values $l = -4$, $l = -2.5$, $l = 1.5$.

We will now examine quantitatively the dependence of the growth rate on β, the Zeldovich number. Recalling that the theoretical dispersion relation is the leading term of an expansion in powers of $(\beta)^{-1}$, we can expect our experimental value of the growth rates σ_{exp} (γ, β, k, l) to be related to the theoretical value $\sigma_{th}(k, l)$ by the relation

$$\sigma_{exp}(\gamma, \beta, k, l) = \sigma_{th}(k, l) + \frac{1}{\beta}\sigma_1(\gamma, k, l) + \frac{1}{\beta^2}\sigma_2(\gamma, k, l) + \ldots$$

Where σ_1 and σ_2 are unknown functions, which could in principle be determined by a theoretical analysis developed up to the next orders. Hence, in the spirit of asymptotics, the difference between our measures and the theoretical values has to behave like $(\beta)^{-1}$ in first approximation. We emphasize that although in the theoretical

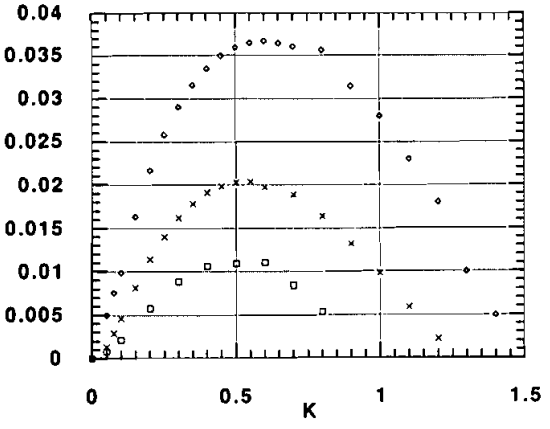

FIGURE 6 $(\sigma_{exp} - \sigma_{th})$ *vs.* wave vector for $\beta = 10$ $\gamma = 0.8$: $l = -1.5$ (squares); $l = -2.5$ (crosses); $l = -4$ (diamonds).

TABLE II
σ_{exp}, $\sigma_{exp} - \sigma_{th}$, $\beta(\sigma_{exp} - \sigma_{th})$ *vs.* β, for $l = -4$, $k = 0.3$ and $\gamma = 0.8$ ($\sigma_{th} = 2.82 \times 10^2$)

β	σ_{exp}	$\sigma_{exp} - \sigma_{th}$	$\beta(\sigma_{exp} - \sigma_{th})$
10	5.79×10^{-2}	2.98×10^{-2}	2.98×10^{-1}
15	4.70×10^{-2}	1.89×10^{-2}	2.83×10^{-1}
20	4.21×10^{-2}	1.40×10^{-2}	2.80×10^{-1}
30	3.68×10^{-2}	0.87×10^{-2}	2.60×10^{-1}

analysis expansions are performed up to $O(\beta)^{-1}$, the dispersion relation obtained at the end of the calculation is only valid to $O(1)$, as explained in Joulin and Clavin (1979).

In Table II, the numerical values of σ_{exp}, $\sigma_{exp} - \sigma_{th}$, $\beta(\sigma_{exp} - \sigma_{th})$ are reported for $l = -4$, $\gamma = 0.8$, $k = 0.3$ (near the maximum growth rate) and different values of β. In Table III, the same quantities are presented for $l = -2.5$, $\gamma = 0.8$ and $k = 0.2$. As expected by asymptotics, the discrepancy between theory and numerical experiment scales approximately like $(\beta)^{-1}$. More precisely, for $l = 4$, $\gamma = 0.8$ and $k = 0.3$, we have approximately $\sigma_{exp} = \sigma_{th}(1 + 10/\beta)$ while for $l = 2.5$, $\gamma = 0.8$ and $k = 0.2$, the behaviour is $\sigma_{exp} = \sigma_{th}(1 + 44/\beta)$ showing the increase of relative error near the theoretical limit $l = -2$.

The study presented above is carried out at k fixed close to the maximum growth rate. Let us now go on with the whole range of unstable wavenumbers. Figure 7 shows a plot of β $(\sigma_{exp} - \sigma_{th})$ *vs.* k for $l = -4$, $\gamma = 0.8$, and two different values of the Zeldovich number ($\beta = 10$ and $\beta = 20$) while Figure 8 shows the same plot for $l = 2.5$. On both figures, the curves corresponding to the different values of β superpose on each other for a wide range of wavenumber, corresponding to those having a high growth rate. The disagreement appearing at very low k or at high k can have two different explanations: either a numerical reason because the numerical precision is very sensitive when computing a correction (especially at low k) or a reason due to the asymptotic expansion itself because terms in $(\beta)^2$ can of course play an important role in this first order correction, especially at high k.

On Figure 9, we tentatively plot $\beta(\sigma_{exp} - \sigma_{th})/(-l - 0.4)$ with respect to k for different values of the control parameter ($l = -4$, $l = -2.5$ and $l = -1.5$) and for different values of the reduced activation energy ($\beta = 10$ and $\beta = 20$). These plots show that all different curves approximately superpose on each others for the most significant range: $k < 0.5$.

This indicates that the function $\sigma_1(\gamma, k, l)$ admits a possible separation of variables, valid on $k < 0.5$ and behaving roughly like $(-l - 0.4)$ for $\gamma = 0.8$. This last expression

TABLE III
σ_{exp}, $\sigma_{exp} - \sigma_{th}$, $\beta(\sigma_{exp} - \sigma_{th})$ *vs.* β, for $l = -2.5$, $k = 0.2$ and $\gamma = 0.8$ ($\sigma_{th} = 0.26 \times 10^2$)

β	σ_{exp}	$\sigma_{exp} - \sigma_{th}$	$\beta(\sigma_{exp} - \sigma_{th})$
10	1.40×10^{-2}	1.14×10^{-2}	1.14×10^{-1}
15	1.00×10^{-2}	0.74×10^{-2}	1.11×10^{-1}
20	8.20×10^{-3}	5.60×10^{-3}	1.12×10^{-1}
30	6.50×10^{-3}	3.90×10^{-3}	1.17×10^{-1}

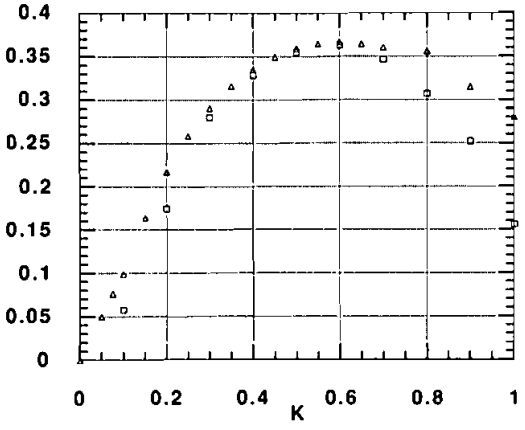

FIGURE 7 $(\sigma_{exp} - \sigma_{th})*\beta$ *vs.* wave vector for $l = -4$ $\gamma = 0.8$: $\beta = 10$ (triangles); $\beta = 20$ (squares).

was found as a result of a fit among other simple possible forms of variation of σ_1 with l.

At this point, we still have to check whether all those results are not specific of the chosen gas expansion parameter. In Table IV, we report results obtained for $\gamma = 0.4$, $l = -2.5$ and $k = 0.2$. They show that, in this case too, the difference $\sigma_{exp} - \sigma_{th}$ scales like $1/\beta$. Of course, as mentioned in Section 4.2, the function $\sigma_1(\gamma, k, l)$ depends on γ. As a result, the coefficient appearing in Table IV is different from the one of Table III.

5 NUMERICAL SIMULATIONS OF UNSTABLE THERMAL-DIFFUSIVE FLAMES

All the results, that we present in this part, are obtained with $\beta = 10$ and $\gamma = 0.8$; We recall that the threshold of the thermal-diffusive instability is attained at $l = -2$, corresponding to Le $= 0.8$ for real flames ($\beta = 10$). The following simulations will be made for $l = -4$, which corresponds here to Le $= 0.6$. The measured numerical

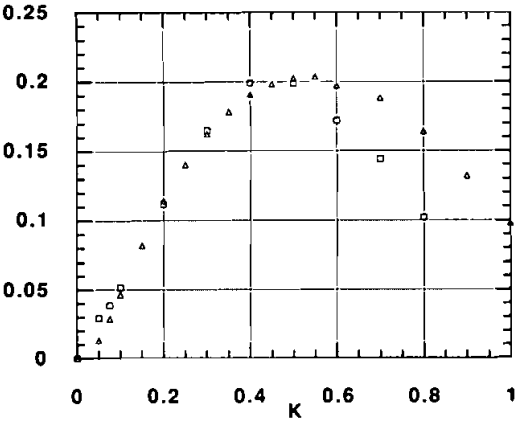

FIGURE 8 $(\sigma_{exp} - \sigma_{th})*\beta$ *vs.* wave vector for $l = -2.5$ $\gamma = 0.8$: $\beta = 10$ (triangles): $\beta = 20$ (squares).

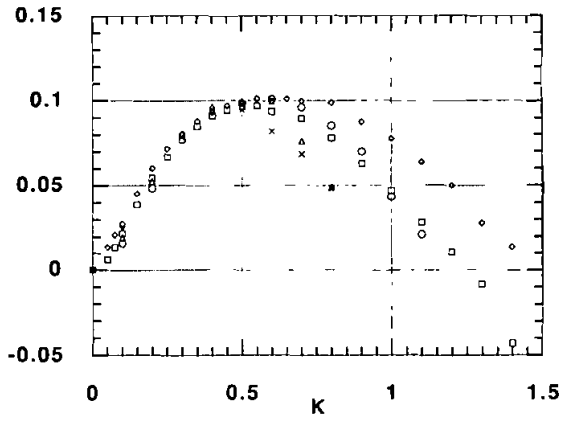

FIGURE 9 $(\sigma_{exp} - \sigma_{th})*\beta/(-l\ -0.4)$ *vs.* wave vector for $\gamma = 0.8$: $l = -1.5$ $\beta = 10$ (triangles); $l = -2.5$ $\beta = 10$ (squares); $l = -2.5$ $\beta = 20$ (crosses); $l = -4$ $\beta = 10$ (diamonds); $l = -4$ $\beta = 20$ (circles).

growth rates are plotted on Figure 3. The typical wavelength is thus more that 15 times as large as the flame thickness which is given by the size of the pre-heating zone. The value $l = -4$ can be considered as being at the limit of the basic assumption of near equi-diffusion $l = O(1)$. Nevertheless we shall obtain an interesting comparison with the KS equation. Although our simulations are carried out in cartesian coordinates, a confinement applied to the y-direction can be interpreted as a laterally finite domain in which the flame propagates. For example, we can have in mind a pipe whose radius has the same typical size. So we will refer to a tube diameter which is the same as the computational width in the y direction.

5.1 *Simulation in Small Pipe*

Let us define L_y as: $L_y = 2Y_0$. This quantity corresponds to the diameter of the tube in which the premixed flame propagates. This image of a pipe is to be interpreted loosely because periodic boundary conditions in the y-direction are not consistent with the presence of duct walls. We intend simply that the picture of propagation in a pipe fixes a lower bound to the wave-numbers allowed to be unstable. This is additionally a source of quantification: *i.e.*, all unstable wave-numbers are integer multiples of the basic quantity given by $k_1 = 2\pi/L_y = \pi/Y_0$. A small tube is then characterized by a diameter allowing a limited number of unstable modes. In this paragraph we choose $L_y = 35.5$ so that only three unstable modes are allowed, as shown in Fig. 10 by the vertical dashed lines. Only k_1, $k_2 = 2k_1$ and $k_3 = 3k_1$ have a positive growth rate according to our measurements, k_2 being more strongly amplified. The numerical experiment we are describing in this paragraph is initiated

TABLE IV
σ_{exp}, $\sigma_{exp} - \sigma_{th}$, $\beta(\sigma_{exp} - \sigma_{th})$ *vs.* β, for $l = -2.5$, $k = 0.2$ and $\gamma = 0.4$ ($\sigma_{th} = 2.60 \times 10^3$)

β	σ_{exp}	$\sigma_{exp} - \sigma_{th}$	$\beta(\sigma_{exp} - s_{th})$
10	9.64×10^{-3}	7.04×10^{-3}	7.04×10^{-2}
15	7.15×10^{-3}	4.55×10^{-3}	6.83×10^{-2}
20	6.03×10^{-3}	3.43×10^{-3}	6.86×10^{-2}

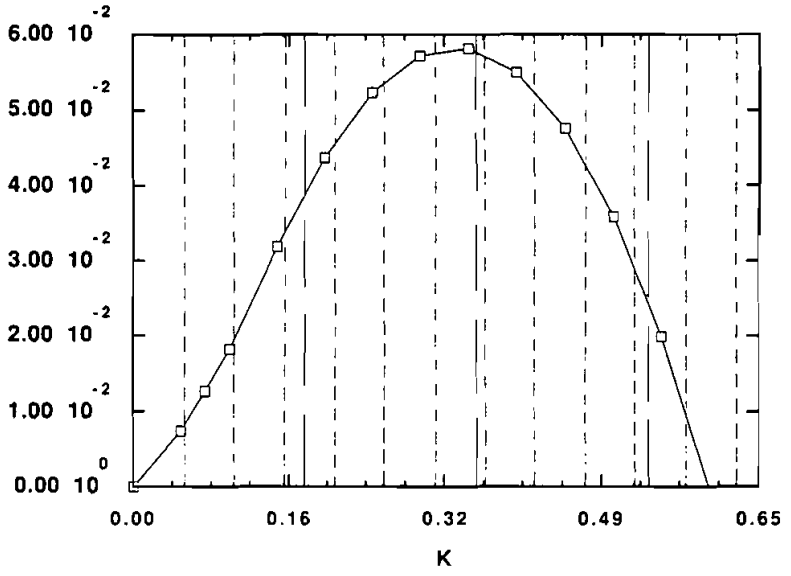

FIGURE 10 Dispersion relation corresponding to the thermo-diffusive instability (measured numerically). The growth rate is plotted *vs.* the wave-number of the perturbation. the parameters are $\beta = 10$, Le $= 0.6$, $\gamma = 0.8$. The dashed lines represent the unstable wave-numbers in a periodic small box of size $L_y = 35.5$. The dotted lines show the allowed modes in a large box of size $L_y = 120$.

with a flat flame front perturbed by a sine function of small amplitude. The wave-number of the perturbation is k_1.

The size of the integration domain has been chosen to be large enough compared to the expected flame corrugation: $X_0 = Y_0 = 0.5\ L_y$. 256 Fourier modes have been selected in the x-direction and 48 in the y-direction. The contour levels of the temperature, drawn on Figures 11(a) to 11(f), show the transient behaviour from the initiation to the steady state obtained after about a hundred time units.

Figure 11(a) illustrates the first stage dominated by the linear behaviour: the initital perturbation has grown accordingly to the linear growth rate. A rather pure sine function is preserved in the first stage of the integration. When the wrinkles have reached a finite amplitude, non-linear saturation occurs in the form of a cusped pattern, as shown in Figure 11(b), composed of a very flat "tip" pointing towards the fresh mixture and of a "cusp" (region with large gradients in the y-direction), pointing towards the burnt gases. Because the tip is a nearly plane region that occupies roughly half of the box, and because diffusive thermal instability is a local phenomenon (as explained in Section 2), the tip becomes unstable with respect to perturbations of wave-number k_2.

Figure 11(c) and Figure 11(d) illustrate the creation of a new "tip". This mechanism can be related to the mechanism of "tip-splitting" occuring in experiments on curved fronts (see Tabeling *et al.* (1987)). The new pattern develops into a steady solution exhibiting a cusped pattern analogous to the first one, as shown in Figure 11(e) and Figure 11(f).

To conclude this part, we have shown that non-linear effects have provoked the initially developed pattern to evolve towards a more stable solution. Thus, it has been found that the k_1 solution is non-linearly unstable or has, at least, a very narrow attractive basin. The two cell solution is the only one to be physically observed. This

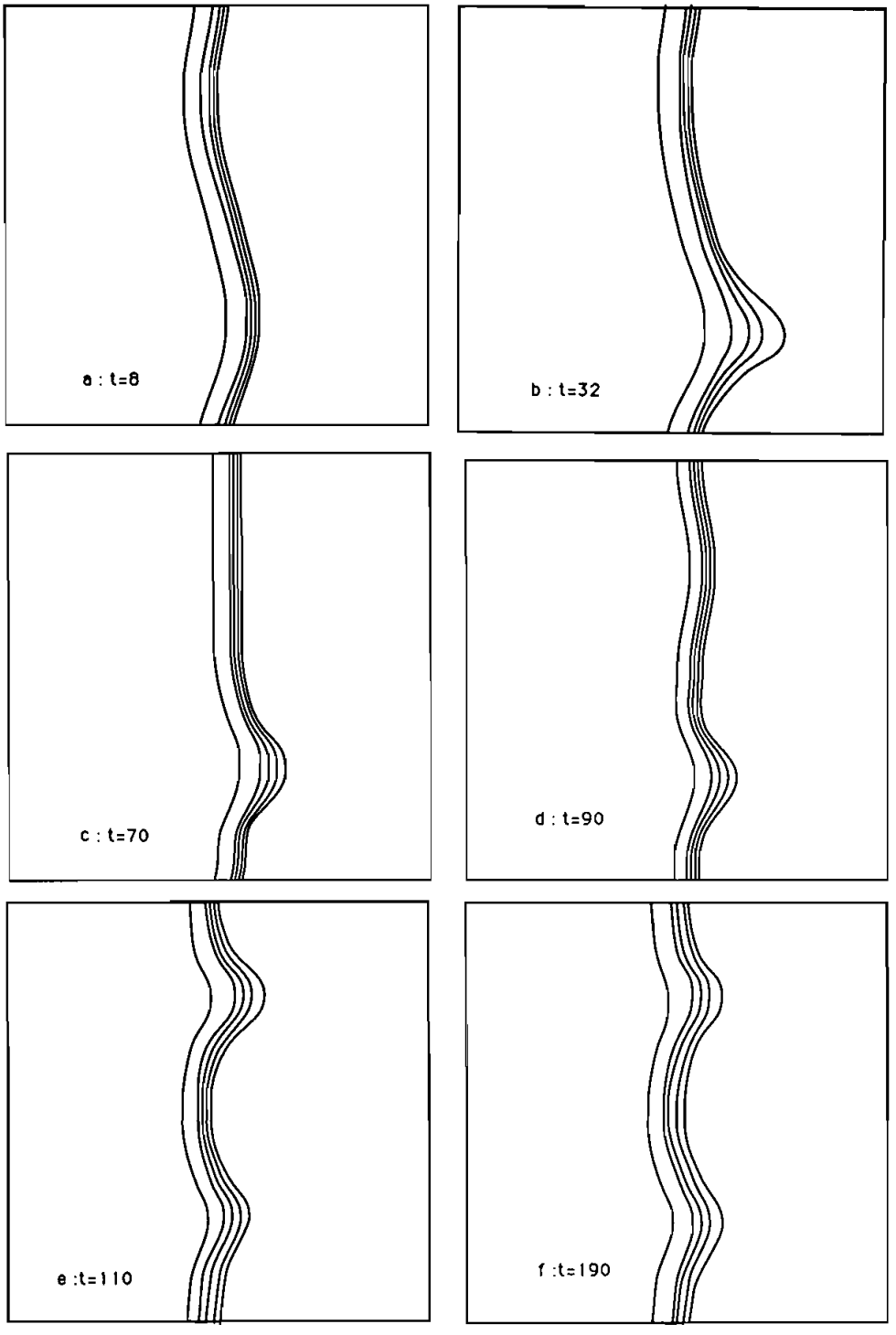

FIGURE 11 Steady solution in a periodic small box: The basic one wave-length disturbance gives way to a two wave-length steady solution. the isotherms are plotted for 6 values of time; (a): $t = 8$, (b): $t = 32$, (c): $t = 70$, (d): $t = 90$, (e): $t = 110$, (f): $t = 190$. The parameters are $\beta = 10$, Le $= 0.6$, $\gamma = 0.8$ and $L_y = 35.5$.

result is qualitatively close to what occurs in the numerical simulations (see Hyman and Nicolaenko (1986)) of the KS equation: steady patterns are obtained in small boxes and are composed of rather small cells whose wave-number of course lies in the unstable range given by the linear analysis.

When the pipe is too small, the dynamics is limited to a competition between only a few modes. If we increase the integration domain in the y-direction we can expect a more interesting behaviour.

5.2 *Simulation in Large Pipe*

Increasing the integration domain amounts to considering that the flame propagates in a larger pipe, in the sense described above. In this paragraph we choose $L_y = 120$ so that 11 unstable modes are allowed, as shown on Figure 10 by the vertical dotted lines. Because we expect an increase in the computational effort, we slightly shorten L_x to $L_x = 20$. Furthermore, 128 Fourier modes are retained in both directions. The numerical experiment we are describing in this paragraph has been initiated with two different types of perturbation of a flat flame front:

5.2.1 *Pure sine function* If the initiation is carried out with eight cells, the wave-number of the perturbation is k_8 and of course lies in the unstable range of Figure 10. However, this perturbation does not have the largest amplification rate.

The time integration shows that such a "clean" initiation can grow by preserving the starting number of cells. This finally leads to a steady state solution exhibiting a regular cusped pattern whose basic wave-number is k_8. The contour levels of the temperature, iso-concentration of the limiting reactant and iso-production lines are drawn on Figure 12(a) to Figure 12(c) showing steady pattern similar to Figure 11(f).

This result is consistent with the integration (see Aimar (1982), Frisch *et al.* (1986)) of the KS equation in a large box, provided that the initalization pattern contains a large number of regular cells. If the number of cells fits with the box size, the non-linear saturation leads to regular flat "tips", small enough to remain stable with respect to the basic linear instability. Hence, steady solutions have non-zero attractive basins.

Conversely, if several wave-numbers are initially excited, one can expect a more complex dynamic because the "tip-splitting" mechanism produces new cells that grow in some parts and decay (or merge) elsewhere.

5.2.2 *Random initial conditions* A way to excite several different modes in our large box, is to initiate the integration with a randomly distributed perturbation of feeble amplitude, imposed to the flat front. After a short while, say $t = 8$, the perturbation is smoothed because high wave-number modes are rapidly damped. Then the wave-numbers within the unstable range of Figure 10 are amplified. Non-linear saturation occurs at about $t = 48$ and leads to the pattern shown on Figure 13(d). This picture shows the temperature field and presents about eight cells of non-equal size. The largest ones have a wave-length close to that of the most strongly amplified mode, while the others are of small size, lying at the limit of the unstable modes.

Instead of evolving to a steady state solution, the pattern then develops in a chaotic way during the time-integration that we have performed. This evolution consists of some continuous process of cell creation and cell annihilation as shown on Figures 13(a) to 13(k). The cell creation appears through what we have already called a "tip-splitting" mechanism: at the tip (the rounded part pointing towards the fresh gases) the curvature is low and locally we are close to a flat front situation. A new cell

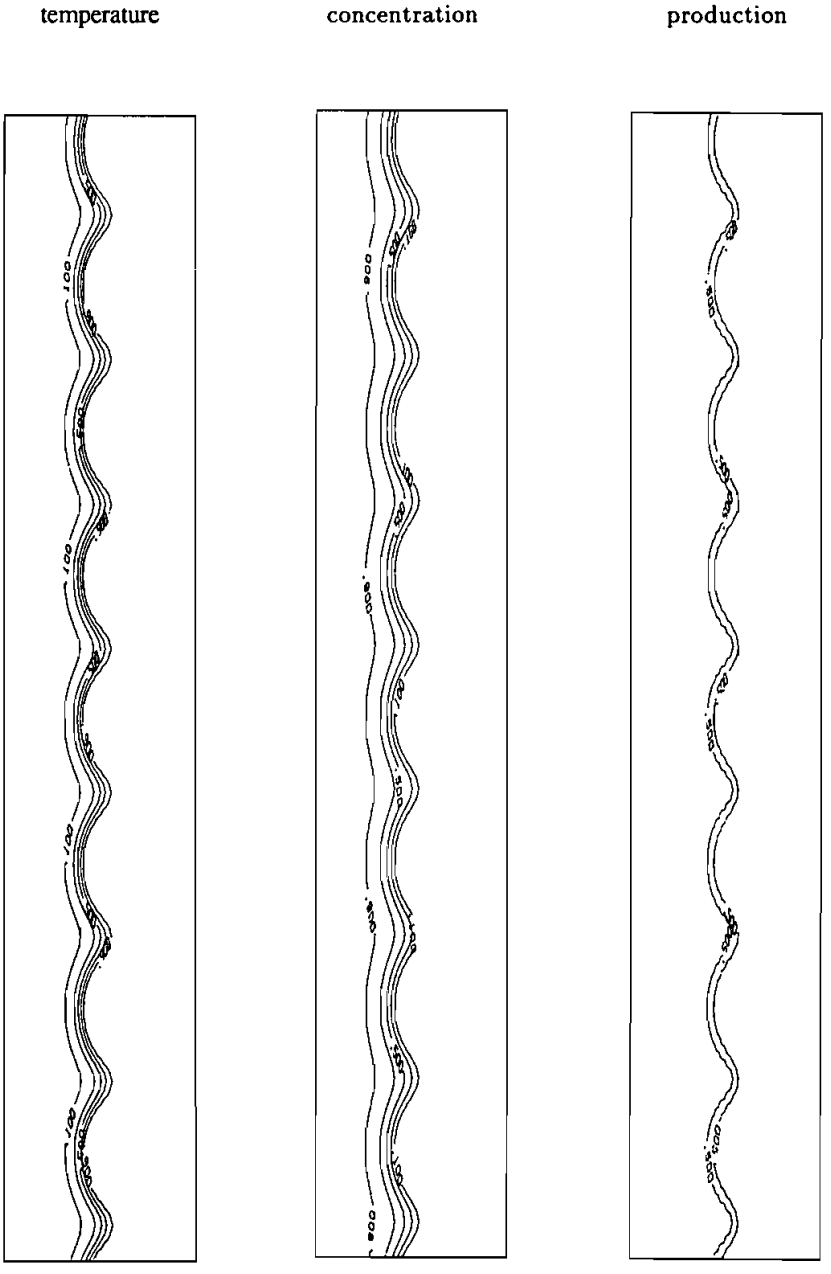

FIGURE 12 Steady solution in a periodic large box: eight wave-length initiation. The problem admits a steady solution provided an acceptable number of regular cells are initiated. Isotherm, iso-concentration and iso-production lines are plotted at the steady state. The parameters are $\beta = 10$, Le $= 0.6$, $\gamma = 0.8$ and $L_y = 120$.

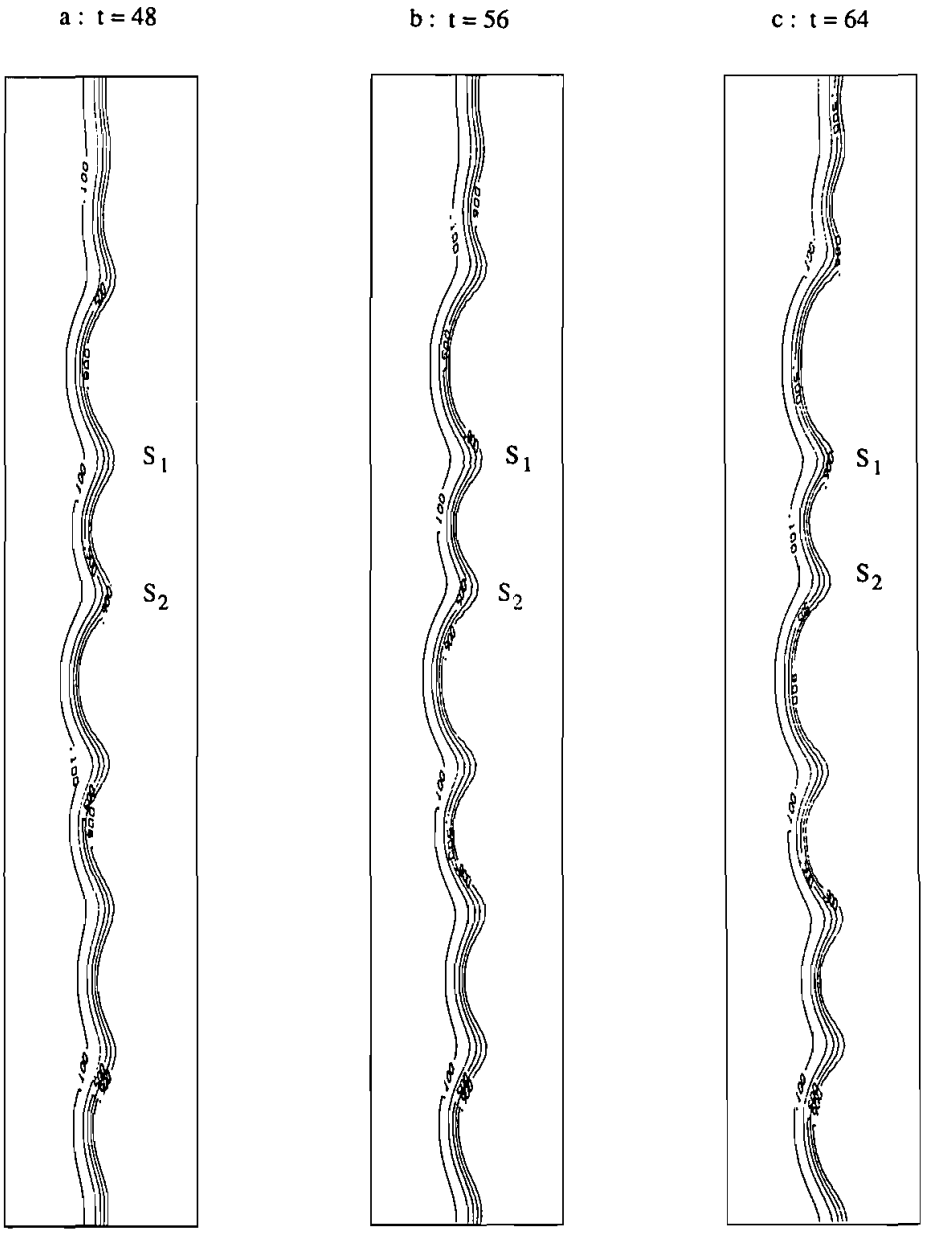

FIGURE 13 Chaotic solution in a periodic large box: random initiation. If a large number of different wave-lengths are initiated, the solution develops into space-time chaos. The isotherms are plotted for 11 values of time: (a): t = 48, (b): t = 56, (c): t = 64, (d): t = 72, (e): t = 80, (f): t = 88, (g): t = 96, (h): t = 104, (i): t = 112, (j): t = 120, (k): t = 128. The parameters are β = 10, Le = 0.6, γ = 0.8 and L_y = 120.

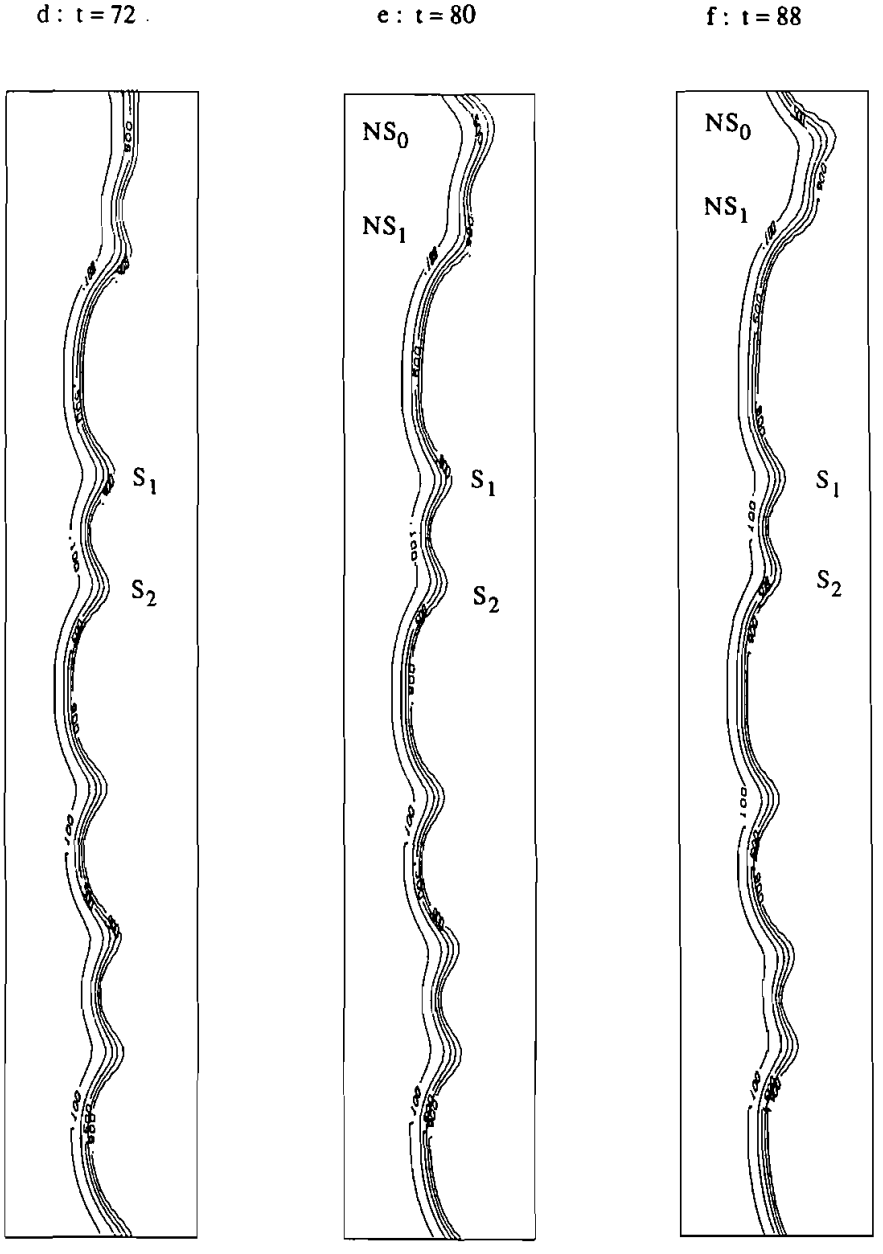

FIGURE 13 continued.

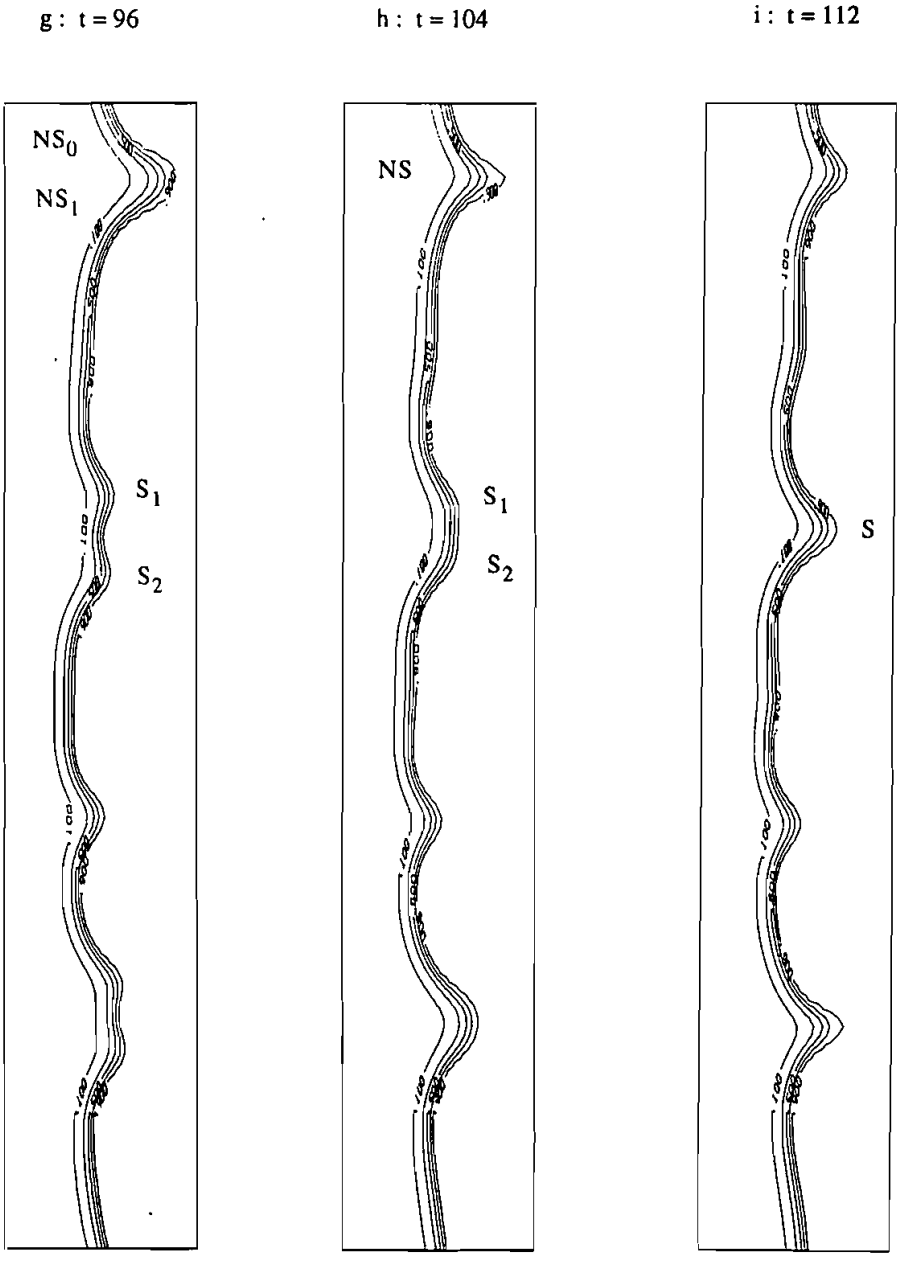

FIGURE 13 continued.

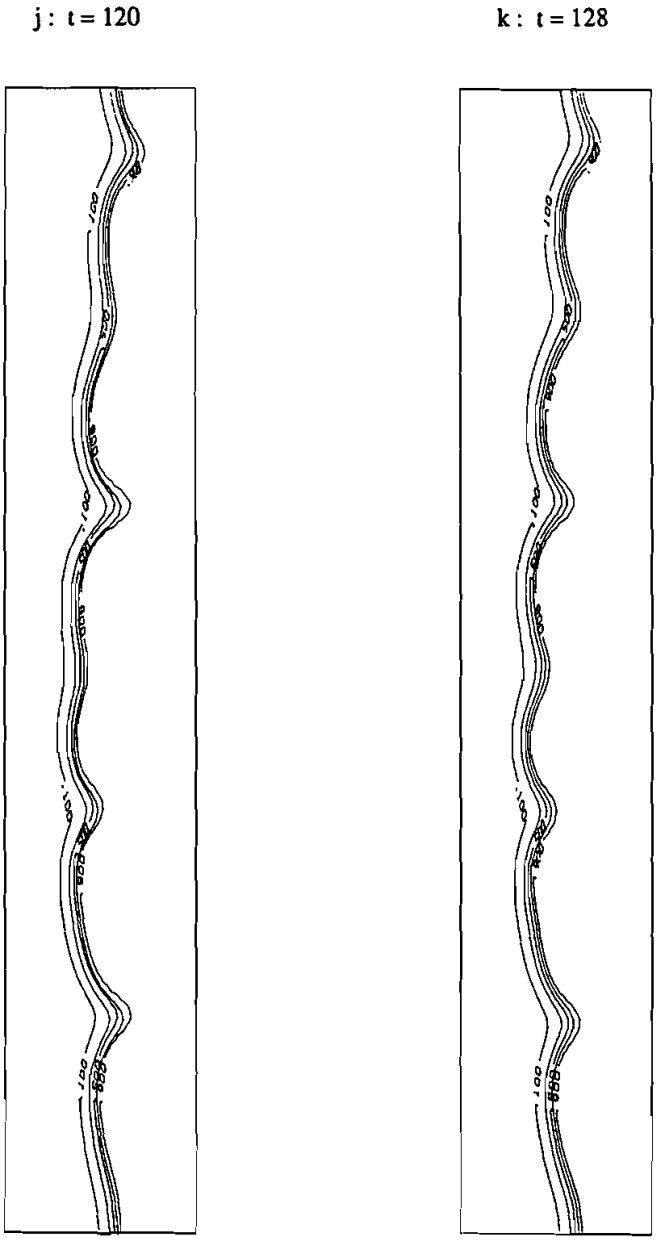

FIGURE 13 continued.

can grow owing to the sensitivity of this portion to the thermal-diffusive instability. The cell annihilation occurs when two cusps merge into a cusp of larger amplitude that afterwards decreases towards the common amplitude. This cusp collision seems to result from two apparently different mechanisms: either two cusps of equal amplitudes are pushed one towards another by the global pattern and merge symmetrically—see *e.g.*, the cusps notes S_1 and S_2 on Figure 13(a) to Figure 13(h); or a cusp of small amplitude seems to be attracted by a larger one and then absorbed in a non-symmetrical way—for instance, the cusp noted NS_1 is quickly "swallowed" by the large amplitude cusp noted NS_0 on Figure 13(e) to Figure 13(g). The latter mechanism could recall the development of the perturbations described by Zel'dovich *et al.* (1980) in the case of curved fronts.

Although this computation ($l = -4$) lies at the margins of the range which is assumed for the derivation of the KS equation, it is striking to observe that the results in a large box exhibit a dynamic qualitatively close to that of the KS equation computed in a large domain with random initial values. For instance, creation and annihilation of cells with the KS equation can be seen clearly in Figure 1 of Shraiman (1986). Computations for even lower Lewis numbers, leading to local extinction phenomenons, can be found in Denet and Haldenwang (1989).

6 CONCLUSION

The present 2-D numerical approach has been able to confirm the dispersion relation obtained from diffusional thermal theory in the high β limit. For finite β, however, the numerically measured growth rates can be rather different from the theoretical ones. Nevertheless, we have shown that the correction, although large, scales like $(\beta)^{-1}$. This result of course remains in accordance with asymptotic analysis.

We also provide a set of original results that allows us to conclude that the qualitative agreement between the experimental observations and the behaviour of the Kuramoto–Sivashinsky equation is not fictitious for flame front dynamics. Furthermore, our results have been obtained in a parameter range for which standard criteria of any weakly non-linear derivation are near their limits. This indicates that the domain of validity—in a qualitative sense—is larger than the one that is usually recognized.

ACKNOWLEDGEMENTS

We wish to thank Professor Paul Clavin who, through extremely helpful advice and encouragements, stood at the origin of the present study.

This work has received support from the scientific commitee of the "Centre de Calcul Vectoriel pour la Recherche" which provided the computational resources.

REFERENCES

Aimar, M. T. (1982). Etude numérique d'une équation d'évolution non linéaire décrivant l'instabilité thermo-diffusive d'une front de flamme. Thesis, Université de Provence.

Barenblatt, G. I., Zeldovich, Y. B., and Istratov, A. G. (1962). On diffusional thermal stability of laminar flames. *Prikl. Mekh. Tekh. Fiz.* **2**, 21.

Bayliss, A., Matkowsky, B. J., and Minkoff, M. (1989). Numerical computation of bifurcation phenomena and pattern formation in combustion. In "Numerical combustion", Lecture Notes in Physics, Dervieux A. and Larrouturou B. Ed., Springer Verlag, vol. **351**, 187–198.

Benkhaldoun, F. and Larrouturou, B. (1991). A finite element adaptive investigation of two dimensional flame front instabilities. To appear in *Comp. Meth. in Appl. Mech. Eng.*

Bregeon, B., Gordon, A. S., and Williams, F. A. (1978). Near limit downward propagation of hydrogen and ethane flames in oxygen nitrogen mixtures. *Combust. Flame* **33,** 33–45.

Buckmaster, J. D. and Ludford, G. S. S. (1983). Lectures on Mathematical Combustion, (SIAM-CBMS, Philadelphia).

Canuto, C., Hussaini, M. Y., Quarteroni, A., and Zang, T. A. (1988). Spectral Methods in fluid Dynamics. Springer-Verlag, Berlin.

Clavin, P. (1985). Dynamic behaviour of premixed flame fronts in laminar and turbulent flows. *Prog. energy Combust. Sci.* **11,** 1–59.

Clavin, P. and Williams, F. A. (1982). Effects of molecular diffusion and of thermal expansion on the structure and dynamics of premixed flames in turbulent flows of large scale and low intensity. *J. Fluid Mech.* **116,** 251.

Denet, B. and Haldenwang, P. (1989). A local extinction of the thermo-diffusive premixed flame at low Lewis number. In "Numerical combustion", Lecture Notes in Physics, Dervieux A. and Larrouturou B. Ed., Springer Verlag, vol. **351,** 223–232.

Denet, B. and Haldenwang, P. (1991). Numerical study of premixed flame Darrieus-Landau instability, submitted to *Combust. Sci. Tech.*

Frisch, U., She, Z. S., and Thual, O. (1986). Viscoelastic behavior of cellular solutions of the Kuramoto Sivashinsky model. *J. Fluid Mech.* **168,** 221–240.

Guillard, H. Larrouturou, B., and Maman, N. (1987). Numerical investigation of two dimensional flame front instabilities using pseudo spectral methods., *INRIA Report* 721.

Hyman, J. M. and Nicolaenko, B. (1986). *Physica D,* **18,** 117–126.

Hyman, J.M, Nicolaenko, B., and Zaleski, S. (1986). Order and complexity in the Kuramoto Sivashinsky model of weakly turbulent interfaces, *Physica D* **23,** 265–292.

Joulin, G. and Clavin, P. (1979). Linear stability analysis of non adiabatic flames: diffusional thermal model. *Comb. Flame* **35,** 139–153.

Kailasanath, K., Oran, E. S., and Boris, J. P. (1989). Numerical simulations of flames and detonations. In "Numerical combustion", Lecture Notes in Physics, Dervieux A. and Larrouturou B. Ed., Springer Verlag, vol. **351,** 223–232.

Macintosh, A. C. and Clark, J. F. (1984). Second order theory of unsteady burner anchored flames with arbitrary Lewis number, *Combust. Sci. Tech.*, **38,**: 161–196.

Margolis, S. B. and Williams, F. A. (1989). Diffusional thermal instability of a solid propellant flame, *SIAM J. Appl. Math.* **49**(5), 1391–1420.

Pelcé, P. and Clavin, P., (1982). The influence of hydrodynamics and diffusion upon the stability limits of laminar premixed flames. *J. Fluid Mech.* **124,** 219.

Peters, N. and Warnatz, J. (Ed.) (1982), *Notes in numerical fluid mechanics 6*, Vieweg.

Quinard, J., Searby, G., and Boyer, L. (1984). Cellular structures of premixed flames in uniform laminar flow . In "Cellular structures in stabilities", Lecture Notes in Physics, Weisfreid J. E. and Zaleski S. Ed., Springer Verlag, vol. **210,** 331–341.

Sabathier, F., Boyer, L., and Clavin, P. (1981). Experimental study of weak turbulent premixed flame. *Prog. Aeronaut. Astronaut.* **76,** 246–258.

Shraiman, B. I. (1986). Order, disorder and phase turbulent., *Phys. Rev. Lett.* **57**(3), 325–328.

Sivashinsky, G. I. (1977). Diffusional thermal theory of cellular flames, *Combust. Sci. Tech.* **15,** 137–145.

Sivashinsky, G. I. (1983). Instabilities, pattern formation and turbulence in flames. *Ann. Rev. Fluid Mech.* **15,** 179–199.

Smooke, M. D. and Koszykowski, M. L. (1986). Two dimensional fully adaptive solutions of solid solid alloying reactions. *J. Comput. Phys.* **62,** 1–25.

Tabeling, P., Zocchi, G., and Libchaber, A. (1987) *J. Fluid Mech.* **177,** 67–82.

Williams, F. A. (1985). Combustion Theory, The Benjamin/Cummings Publishing Company.

Zeldovich, Y. B., Istratov, A. G., Kidin, N. I. and Librovitch, V. B. (1980). Flame propagation in tubes: hydrodynamics and stability. *Combust. Sci. Tech.* **24,** 1–13.